Monitoring Temporal Sandbar and Shoreline Changes at Saint Louis, Senegal: Using Sentinel-2 Imagery (2015–2022)

Adélaïde Taveneau, Rafael Almar, Erwin W. J. Bergsma, Cheikh Omar Tidjani Cissé, Boubou Aldiouma Sy, Abdoulaye Ndour

remote sensing

MDPI

Article

Monitoring Temporal Sandbar and Shoreline Changes at Saint Louis, Senegal: Using Sentinel-2 Imagery (2015–2022)

Adélaïde Taveneau [1,*,†], Rafael Almar [1,†], Erwin W. J. Bergsma [2], Cheikh Omar Tidjani Cissé [3], Boubou Aldiouma Sy [4] and Abdoulaye Ndour [5]

[1] Institut de Recherche Pour le Développement, LEGOS (IRD/CNRS/CNES/Université de Toulouse), 31400 Toulouse, France; rafael.almar@ird.fr
[2] Centre National d'Etudes Spatiales (CNES), 31400 Toulouse, France; erwin.bergsma@cnes.fr
[3] Laboratory of Dynamics and Integrated Management of Coastal Areas (UQAR), 300 Ursuline Path, P.O. Box 3300, Rimouski, QC G5L 3A1, Canada; cheikhomartidjani.cisse@uqar.ca
[4] Leidi Laboratory, Department of Geography, Territorial Dynamics and Development, Université Gaston Berger (UGB), SN-SL, Saint Louis 46024, Senegal; boubou-aldiouma@ugb.edu.sn
[5] Laboratory of Sedimentology, Department of Geology, Faculty of Sciences and Technics, Université Cheikh Anta Diop (UCAD), SN-DK, Dakar 12500, Senegal; abdoulaye17.ndour@ucad.edu.sn
* Correspondence: adelaide.taveneau@ird.fr
† These authors contributed equally to this work.

Abstract: Understanding beach dynamics, both in time and in space, is paramount to better understand how and when to intervene to improve coastal management strategies. Beach morphodynamics is expressed in a variety of ways. As indicators of beach change, we can measure the shoreline, the beach topography, and the bathymetry; e.g., in situ measurements rarely cover large extents, are often collected on a local scale (beach), and rarely cover a sufficient time span with a sufficient surveying frequency or a simultaneous measurement of the beach and bar system. Regular-revisit satellites, such as the ESA's Sentinel-2 mission, provide the opportunity to regularly monitor both shoreline and sandbar dynamics, and the time span is increasing and likely to continue for the decades to come. Using the satellite-derived shoreline and bar position, here, we show that the shoreline and bar are intrinsically coupled. Using Sentinel-2 satellite imagery, we show that the actual erosion/accretion status of the beach at Saint Louis (Senegal) is strongly influenced by the sandbar dynamics. There is a coupled behavior in their seasonal evolution and trend. Our results show that a very large accretive wave of about 50 m observed on the beach is driven by a local welding of the inner sandbar to the beach. Finally, we conclude that this type of event could be anticipated by an analysis of the sandbar.

Keywords: satellites; nearshore sandbar; landward migration; coastal engineering

Citation: Taveneau, A.; Almar, R.; Bergsma, E.W.J.; Cissé, C.O.T.; Sy, B.A.; Ndour, A. Monitoring Temporal Sandbar and Shoreline Changes at Saint Louis, Senegal: Using Sentinel-2 Imagery (2015–2022). *Remote Sens.* **2024**, *16*, 3551. https://doi.org/10.3390/rs16193551

Academic Editor: Deepak R. Mishra

Received: 21 June 2024
Revised: 17 September 2024
Accepted: 21 September 2024
Published: 24 September 2024

1. Introduction

Nearshore sandbars are morphological features that generally characterize sandy and wave-dominated shores [1–3]. Located in the surf zone, they are the result of a combination of sediment transport induced in cross-shore and longshore directions [4]. Their shape—which depends on environmental conditions and sediment characteristics—varies widely from linear to three-dimensional features and was first classified in [5]. This classification was based on observations of a large panel of single sandbars, micro-tidal coastal areas, and allows for defining a beach as reflective, dissipative, or intermediate. It is even possible to observe numerous bar morphologies on the same intermediate beach [6,7]. In natural environments, sediment fluxes never reach equilibrium because the morphological response of the sandbar(s) is generally longer than the time scales associated with changes in the wave regime: this leads to a landward or seaward shift of existing sand structures. This morphological evolution of a littoral system associated with sandbar dynamics is the main source of profile variability on short (sub-seasonal scale), medium (seasonal scale), and long (inter-annual scale) time scales [8].

The sandbar system plays a key role in the sustainability of the aerial beach, and beach conservation at urban coasts, as it reduces the energy of the incoming wave: as the waves arrive at the shore, they break on these features and some of their energy is dissipated so that when they reach the shore, they are less energetic and, therefore, less erosive. Their longshore dynamics have been shown to be highly correlated with the upper beach [9–11], and the wave conditions are the main driver of their short-term cross-shore dynamics. During very energetic episodes (e.g., storms), the sandbars migrate rapidly seaward with migration rates of up to 10 m/day [12,13] due to the feedback between the bottom and the seaward sediment fluxes induced by the undertow. Conversely, sandbars migrate slowly shoreward under low to medium energy wave conditions with velocities of about 1 m/day [1] due to the feedback between the bottom and the seaward sediment fluxes induced by the orbital velocity non-linearities [14]. The position of a sandbar—given the seasonal variability of the swell climate—is farther from the shore during energetic wave conditions than during moderate conditions. Some sandy beaches also have a double bar system, which shows cyclical behavior on inter-annual scales: net offshore migration of the whole bar system (see [11,12,15,16]). When the outer bar reaches a limit depth, it begins a degeneration phase that leads to the inner bar becoming the new outer bar. At the same time, a new (inner) bar is formed near the coastline.

In a large number of coastal areas, bathymetric information is unavailable or, in most cases, decades old. These bathymetries are extremely useful for constraining coastal sea state models [17]. Space observations are an important complement to existing terrestrial and airborne observing systems, with the advantage of systematic monitoring [18,19]. Satellites provide unparalleled spatial coverage of every coastline in the world with high spatial resolution [17,20]. Data are collected regularly with unrestricted access to any coastline in the world (without natural or administrative access restrictions), allowing for temporal monitoring, unlike highly demanding field observations, which are necessarily limited in space and time. The Saint Louis coast, with its unique and challenging environmental conditions [21,22], has not been extensively studied in terms of nearshore sandbar dynamics. The present study aims at contributing at filling a critical gap in understanding the coastal processes in this region.

Similarly, shoreline detection involves identifying transitions in pixel intensity across multiple spectral bands and is a common technique in coastal video monitoring [23,24]. Luijendijk et al. (2018) [25] utilized Landsat data in combination with the Digital Shoreline Analysis System (DSAS) to assess global shoreline changes, emphasizing the value of Landsat's extensive temporal coverage. Similarly, using different techniques, several studies [26–29] demonstrated the use of Sentinel-2 in capturing subtle changes in shoreline positions at sandy beaches. Machine learning techniques are increasingly being integrated with remote sensing data for predictive modeling of shoreline changes. These approaches can handle large datasets and identify complex patterns that might be missed by traditional methods. For example, ref. [30] combined Landsat imagery with machine learning algorithms to predict shoreline retreat in response to sea-level rise. In a different approach, ref. [31] employed a Support Vector Machine (SVM) algorithm to classify and predict shoreline changes using Sentinel-2 data, demonstrating the effectiveness of machine learning in improving the accuracy of shoreline change predictions.

Regarding sandbar, the technique of optically remotely deriving the location of natural sandbars based on the dissipation of wind waves and swell over the bar crest was first introduced by [6]. Using the satellite's Red–Green–Blue color bands, the sandbar is identified based on the foam generated by the breaking wave—provided the waves have sufficient energy. This approach emphasizes the white color through pixel intensity derived from the averaged RGB bands of satellite imagery. Consequently, the sandbar is clearly highlighted and manually digitized—a method similar to the Argus camera monitoring system [32]—ensuring an accurate representation of its morphology. The method for detecting the maximum intensity signatures of waves breaking on sandbars is now widely used in coastal video monitoring [1,11,13], among others. Similar to shoreline, while sandbars

have historically been monitored using video shore-based techniques [1,33,34], there is a growing interest in using satellite imagery from its global availability and its potential, in particular in a context of increasing revisit and resolution [35] and in particular at poorly documented stretches of coast such as West Africa [36]. Only a few studies have employed satellite imagery to monitor sandbar morphodynamics on a regional scale, offering valuable insights into coastal processes. For example, SPOT (Satellite Pour l'Observation de la Terre) images, combined with in situ wave measurements, were utilized to track sandbar migration between 1986 and 2000, demonstrating the capability of satellites to monitor these features over extensive temporal scales in regional contexts [37]. A notable innovation in current research is the use of global and regular revisit Landsat and, more recently, Sentinel-2 imagery to track nearshore sandbars [38–41], a relatively new approach, particularly in the context of coastal morphodynamic studies in West Africa. These advancements underscore the significant role of satellite optical imagery in enhancing our understanding of sandbar dynamics and supporting effective coastal management. Here, the manual digitization of sandbar and shoreline positions based on visual inspection of wave-induced foam and spectral band transitions, while a known technique, is applied to insure a high level of precision and in a challenging coastal environment.

In coastal management, decisions are often guided by an understanding of changes in sediment volume over time and space [42]. In this study, we investigate the potential of high-frequency satellite imagery, specifically Sentinel-2, to track nearshore submarine sandbars both temporally and spatially. The primary objective is to understand the dynamics of nearshore sandbars along the Saint Louis coast, focusing on their temporal and spatial evolution, particularly in response to seasonal wave climate variations. Previous studies in the literature have not identified the presence of submarine sandbars along the Saint Louis coast. This research aims to investigate the morphodynamics of these sandbars, tracked using Sentinel-2 satellites, and to explore their potential connection with the coastline and sandspit dynamics. This study aims to determine how the position and movement of sandbars influence the shoreline, with an emphasis on understanding the coupled dynamics between these two features. Using both satellite imagery and observations on the field allows for capturing phenomena that are not visible when one is looking at the regional or local scale only. A key objective is to link observed sandbar behaviors to broader coastal processes, including erosion and accretion patterns, and to assess the implications for coastal management in the region. This application is particularly relevant to our application case here, Saint Louis, Senegal, where information on submerged sandbars is currently lacking and is therefore crucial [36].

2. Study Site

Saint Louis—located in northern Senegal (West Africa)—presents the particularity of being built on a very dynamic sandspit named the Langue de Barbarie (Figure 1). Erected between the Senegal River and the Atlantic Ocean, this city faces both marine hazards (coastal erosion [21,43], coastal flooding [44]) and hydrological issues (flooding, turbidity). It is a place with very energetic conditions: swell mainly comes from the NNW direction (the mean wave height H_S = 1.52 m and the mean peak period T_P = 9.25 s [22]) obliquely to the shore, leading to one of the strongest longshore sediment transports in the world (about 800×10^3 m^3/year [45]). Because of its low latitude, Senegal has a seasonal system with two distinct periods: the dry season (from November to May) and the rainy season (from June to October) [22]. It is also influenced by distant swells in the North Atlantic, with the calm of the summer and the energetic storms of the winter [45]. This site is unfortunately known for the rapid erosion it faces: rates of −4.2 m/year have been recorded after 2003 [43]. Indeed, 2003 is a key date for Saint Louis: due to a major flood that occurred in October, the water level in the streets was so high that an urgent decision making was required. A breach was initiated in the sandspit for the water to drain away as the river mouth was nearly 30 km away from the city. The breach, which was 4 m wide, rapidly became the new river mouth, and the downdrift part slowly collapsed.

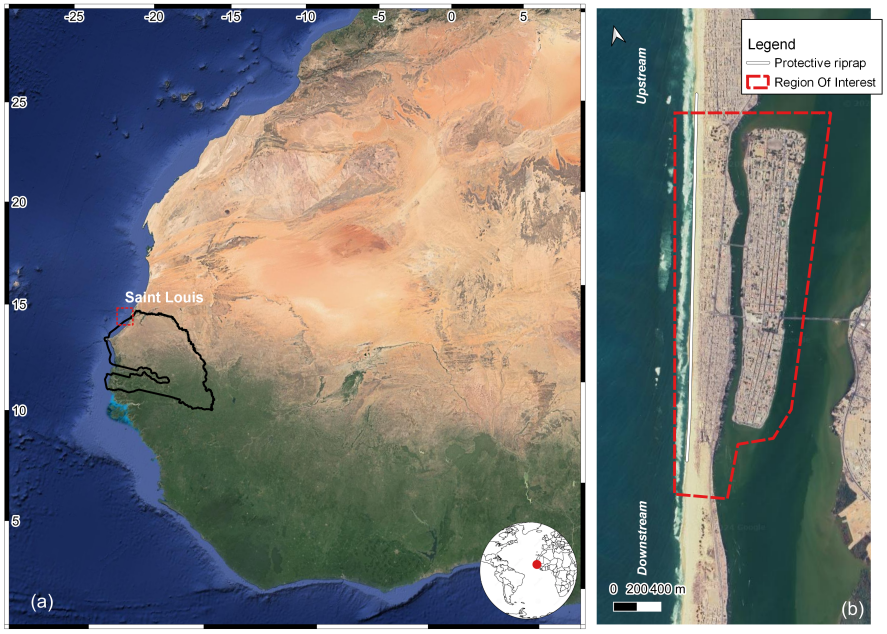

Figure 1. (**a**) Location of the study site (Saint Louis, Senegal, West Africa) on a Google Earth Engine satellite image and (**b**) zoom on the Langue de Barbarie sandspit with a highlight (red dashed outline) on the region of interest (ROI) and the protective riprap location (white line).

The sandspit length rapidly decreased from 30 km to about 10 km, and its southward elongation has since been initiated [22,46,47]. The erosion pattern facing the city of Saint Louis (black square; Figure 1) has been linked to the response of the sandspit to the 2003 breach [20,48]. Indeed, for wave-dominated sandspits, the negative feedback of the sandspit lengthening process is the erosional trend it creates in the updrift part [49,50]. In late 2020, the construction of a 20 km long protective riprap began in front of the most vulnerable and the most densely populated district (Guet Ndar). Since 2021, where an erosive pattern was expected, the beach width has suddenly and significantly increased: which of these mechanisms is responsible for this massive and local beach widening?

3. Methods and Data

3.1. Satellite Imagery

Sentinel-2 imagery was extracted using the Google Earth Engine (GEE) platform, which provides access to publicly available optical satellite imagery. As part of the European Copernicus program, Sentinel-2A and Sentinel-2B were launched in 2015 and 2017, respectively. These satellites provide optical imagery revisit frequencies ranging from every 5 days at the equator to more frequent revisits at higher latitudes, facilitating detailed coastal studies [51]. The ground sampling distance remains constant over time, with a maximum resolution of 10 m for color bands, used in this study for visual inspection and digitization (see Section 3.2), and 20 m for the short-wave infrared (SWIR) band. The regular revisits of Sentinel-2 satellites provide a wealth of data, and the locations of sandbars can be derived from satellite imagery by identifying the foam induced by waves breaking on them. The satellite Level-2A imagery (preferred product for most applications that require surface reflectance) used in this study has not undergone any further correction as it is ortho-rectified by the data provider. Only clear-sky images were utilized by the human operator, which is quite common along this stretch of the Sahel coast near the Sahara Desert, where the dominant trade winds prevail.

In addition, a Pleiades image acquired in March 2019 is employed for comparison purposes. The Pleiades constellation consists of two satellites orbiting out of phase at an altitude of 694 km. These satellites offer on-demand very-high-resolution imagery, providing panchromatic and multispectral outputs with resolutions of 0.25 m per pixel and 2 m per pixel, respectively.

3.2. Sandbar and Shoreline Position Extraction

At Saint Louis, under suitable wave conditions, waves break on the inner bar, leading to visible foam in images. Additionally, during highly energetic wave climates, waves may also break on the outer bar. To insure the continuity of the collected data, the sandbar crest position is captured as follows: if a new sandbar is generated at the coast and appears in the images, its position is tracked until this inner sandbar eventually becomes the outer bar and a new inner bar is generated. Following the approach in [1], here, a matrix $X(t, y)$ is created for both bars, comprising the bar crest locations in the cross-shore direction X at time t and alongshore location y.The remotely sensed bar crest position also varies over time due to fluctuations in offshore waves and tidal levels [52], even if the bar crest itself remains stationary. To account for this artificial migration, we applied the methodology proposed in [53].

While it is generally applied to video-derived time-averaged images, here, satellites provide an instant of the wave breaking and cannot smooth out individual waves. This results in an inherent uncertainty of the order of a wavelength and swash excursion for the sandbar location and shoreline, respectively. To smooth out the inherent noise of individual images, the shoreline and sandbar positions are 3 months averaged to highlight their seasonal and interannual behavior. For a better visualization, the 0 value on the cross-shore position corresponds to the most inland position of the shoreline.

3.3. Ground Truth Validation Dataset and Wave Reanalysis

The sparse in situ data available for validating the satellite-derived sandbar positions at Saint Louis should be acknowledged. This scarcity is part of the motivation of this research, which fills a critical gap in understanding the coastal processes in this region. A validation dataset is derived from a complete topo-bathymetry of the Langue de Barbarie sandspit, acquired in early 2019 (January to February), and a Pleiades satellite acquisition (March 2019). The topo-bathymetry has a decimetric error and was collected by Shore Monitoring and Research and made available for our research, thanks to the Senegalese Agence de Développement Municipal (ADM). Due to the sparseness of in situ data, the in situ sandbar position is derived from both the field measurement and a 03/2019 Pleiades satellite image—2 m resolution—assuming that the sandbar morphology has not evolved between the field measurement and the satellite acquisition (Figure 2).

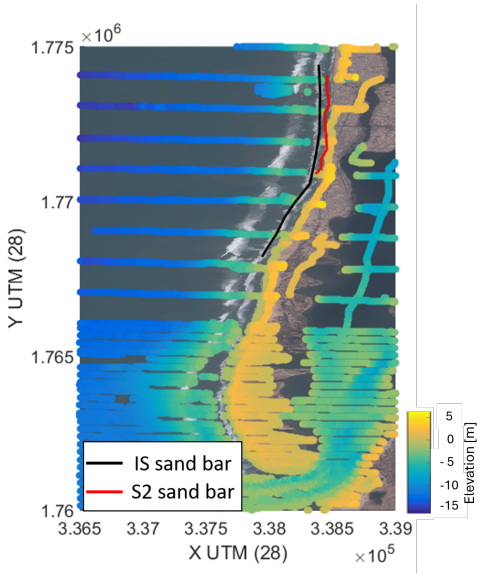

Figure 2. The topo-bathymetry survey conducted in January 2019 (made available from Shore Monitoring and Research) is overlaid on a Pleiades image from March 2019 to evaluate the uncertainty on the satellite-derived sandbar location. The Sentinel-2 sandbar-derived location is shown as a red line; the black line represents the in situ sandbar location.

Although this study uses a validation dataset from 2019 topo-bathymetry, the methodology would benefit from more frequent and widespread validation efforts, particularly to account for the uncertainties in satellite-derived data.

Offshore wave data were obtained from the ERA5 global reanalysis database, which uses a coupled wave-atmosphere model that has been widely used and validated [54]. The data are produced by the European Centre for Medium-Range Weather Forecasts (https://www.ecmwf.int, accessed on 1 October 2022).

4. Results

4.1. The Sandbar–Shoreline Coupled System at Saint Louis: Seasonal Cycle and Trend

Senegal shows a seasonal pattern characterized by two distinct periods—the dry season (from November to May) and the wet season (from June to October). This biannual seasonal cycle exerts a significant influence on the marine climate and, consequently, on the coastline, whose morphology is particularly affected by these seasonal variations. The Senegalese coasts experience a notably energetic wave climate (Figure 3), with an average significant wave height (H_S) of 1.68 m and a period (T_P) of 8.32 s. In particular, there are distinct differences between the two seasons when analyzing the wave spectra: during the dry season, waves tend to be more energetic and predominantly originate from the NNW direction, while during the wet season, the wave directions are more varied.

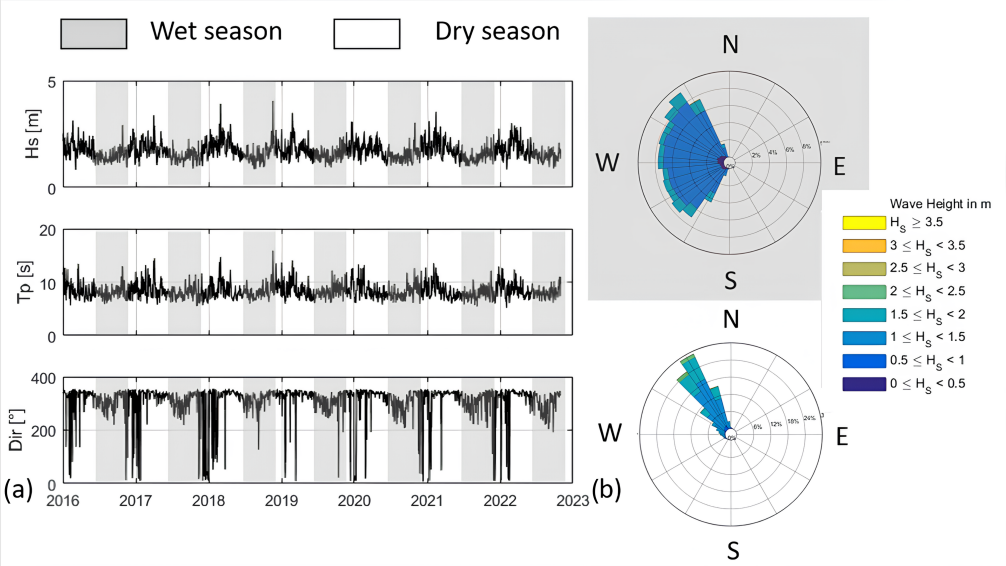

Figure 3. (**a**) Wave parameter time series over the period of interest and their (**b**) associated wave spectra [55]. The data come from the ERA5 reanalysis [54].

Notably, there is a lack of literature describing the nearshore sandbar system at Saint Louis. With its medium sediment size (0.21 mm) and the energetic wave forcing [56], the Saint Louis coastline features have a double bar system that can be identified in satellite imagery (see Figure 4) by the foam generated during wave breaking. This study aims to characterize this system and investigate the relationship between the bars and shoreline dynamics.

The double bar system consists of a highly dynamic inner bar, which is the closest to the shore, and an outer bar whose dynamics decrease with depth. The whole system is characterized by a strong seasonal cycle. The dry and wet seasons significantly influence the dynamics of both the coastline and the inner bar. During the dry season, the shoreline experiences erosion, whereas during the wet season, it expands (see Figure 5; black line). The situation is more complex for the inner bar: during the dry season, the bar shows strong three-dimensional characteristics, whereas it appears more linear when the wave climate is less energetic (see Figure 4). In addition, the mobility of the inner bar is considerably larger than that of the shoreline (see Figure 5; red line), indicating its rapid dynamics and cyclicity.

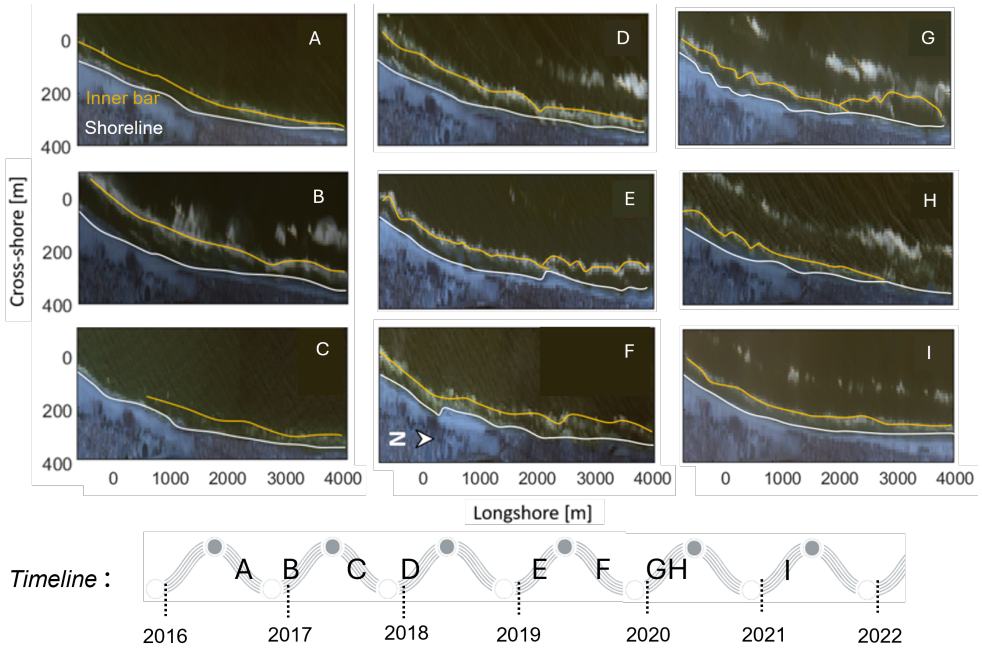

Figure 4. (**A**–**I**) Selected Sentinel-2 images of the study area near Saint Louis City depict the shoreline and sandbar features at different times (timeline below). To enhance clarity, the shoreline is represented by a white line, while the inner sandbar is highlighted in yellow. The time lapse of these images is shown in the timeline below with the wet season and dry season represented as gray circles and white circles, respectively.

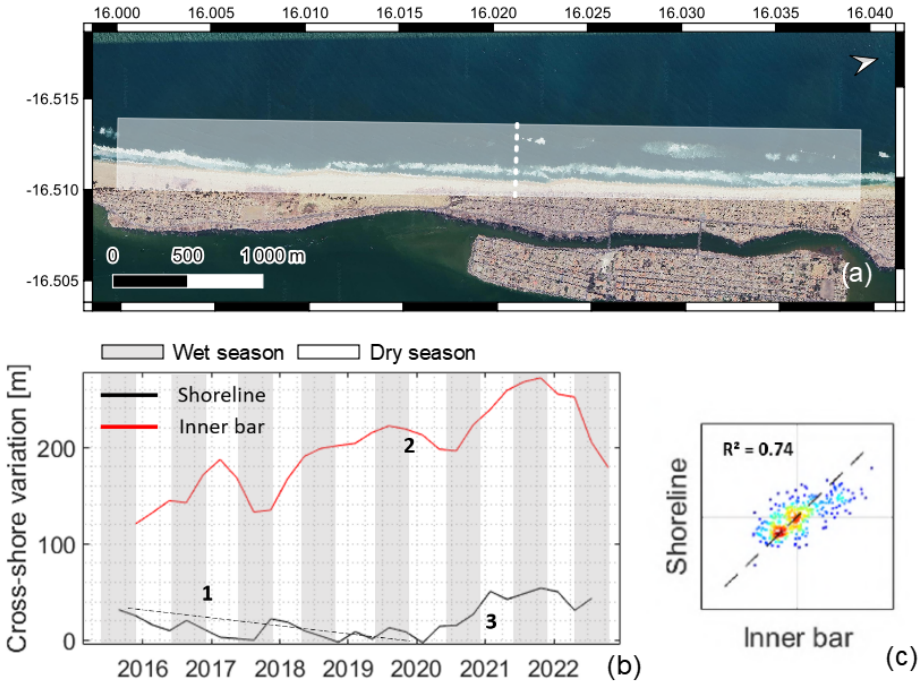

Figure 5. (**a**) Localization of the cross-shore transect (white dashed line) and its alongshore average buffer onto a Google Earth Engine satellite image. (**b**) Three-month longshore averaged time series of the shoreline (black) and sandbar (red) with three points of interest that respectively describe (1) the erosion trend, (2) the shoreward inner bar migration, and (3) eventually the beach accretion. (**c**) Correlation between the inner bar and shoreline position. This transect location is extracted from the ROI defined in Figure 1b.

The time series of the shoreline and the inner bar show interdependent dynamics (see Figure 5), with a remarkably high correlation between the two (anticorrelated, with an explained variance $R^2 = 0.74$). Here, the cross-shore positions of both the sandbar and the shoreline are alongshore averaged (over 100 m) values. The correlation reflects the overall relationship between the two evolutions, although this can certainly vary alongshore. As the shoreline position is a response of the sandbar position, it is noted that using a lag of 4 months on the shoreline position slightly improves the correlation between the two studied features' positions ($R^2 = 0.78$).

Since the 2003 breach, an erosion trend has been observed and described in several studies [20,43,47]. The beach facing the anthropized area had eroded rapidly, and a protective riprap—the construction of which began in late 2020—was considered to protect the population. It is noteworthy how different the trends are before the accretion anomaly of 2020 between the natural areas (upstream and downstream; Figure 5) and the urban one (probably due to the buildings preventing a massive shoreline retreat).

4.2. Shoreward Accretion Wave Event: Welding of the Sandbar to the Beach

A massive beach accretion trend of about +40 m was recorded between 2020 and 2021 (Figure 5). To further investigate this sudden accretion phenomenon, and as the wave climate did not show any anomaly during this period (Figure 3), three satellite images were selected Figure 4: one before the accretion (1), one during the accretion (2), and one after the accretion (3). The inner bar migrates landward during the wet season (less energetic conditions) and welds to the shore, contributing to its widening. Seaward migrating sandbars are the most common in the literature; however, four different modes for a sandbar to migrate landward have been identified for a swell-dominated beach: sandbar welding (SW; mode I), which occurs during low-energetic conditions following a moderately energetic winter; a large sandbar becoming a terrace bar (STT; mode II) during a subsequent very low-energetic period; a terrace bar becoming a sandbar (TST; mode III) during moderately energetic conditions; and finally, sandbar splitting (SS; mode IV) [57]. This last mode occurs during low-energetic conditions; the outer bar flattens and follows a net offshore migration (NOM) cycle as the remaining inner section migrates landward. Mode IV corresponds to what happened in Saint Louis: during the wet season in 2019, the sandbar split. The inner bar migrated progressively landward to weld to the shore in 2020 during the wet season. The inner bar migrated landward throughout the year 2020, and we now want to understand whether this accretion is local and only related to the welding to the coast of the inner bar, or whether a phenomenon with a larger spatial extent is at the origin. For this purpose, the shoreline averaged over a distance of 3 km on the longshore axis is studied at three different locations in non-urbanized areas: 2 km north of the city, which we will call the upstream, and 2 km south of the city, which we will call the downstream. From the observed evolution of the trends per area (Figure 6), it is clear that the +50 m accretion anomaly is only found around the urban beach of Saint Louis. While the urban area clearly shows an accretive pattern in 2020, the two others seem to be dominated by an erosive trend over the 2016–2020 period, and a stabilized configuration is observed from 2020 to 2022.

To estimate our method uncertainty, the location of sandbar derived from Sentinel-2 satellite imagery was compared with surveyed data carried out by Shore Monitoring and Survey, in January 2019, combined with Pleiades-derived imagery. It shows that, in fact, the satellite-derived sandbar location has an error that varies from 40 to 50 m compared with the in situ measurement/high-resolution satellite observation. This error is estimated by comparing the in situ sandbar position with the S2 sandbar position of the nearest date (January 2019 for the in situ acquisition and March 2019 for the S2 data). As the ground pixel resolution of the S2 satellite is 10 m/pixel, the overall uncertainties are estimated to be $\pm$50 m for the sandbar position and $\pm$15 m for the shoreline position.

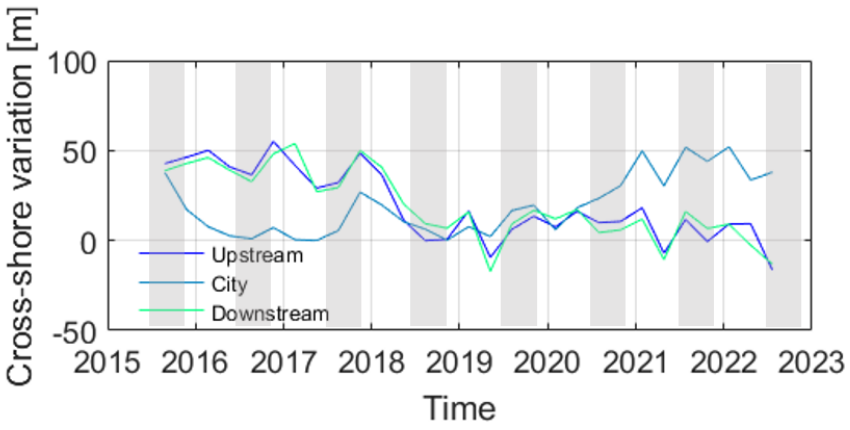

Figure 6. The shoreline was averaged alongshore over a 3 km stretch (smoothed over 3 months) across the entire acquisition period of Sentinel-2 imagery. This analysis was conducted for the upstream region of Saint Louis, the urban area, and the downstream region. Gray areas indicate periods of the wet season, while white areas represent the dry season. The shoreline of the urban beach served as the reference, and the difference between the mean time series of the upstream and downstream areas was calculated to compare trends across all regions.

5. Limitations

Despite this potential, satellite-based methods are still relatively new in this field, in particular for sandbar detection, making the manual extraction process critical to achieving reliable results. The focus of this study is not to develop an automated detection, in part because there is little ground validation at this site, but rather to exploit the potential of existing Sentinel-2 imagery to understand coastal change.

In terms of method uncertainty, foam generated by wave breaking never occurs at the exact location of the wave breaking and varies with waves and tides [1]. Another peculiarity of satellite sandbar location estimation is the instantaneous nature of the acquired imagery compared with conventional time-averaged (typically tens of minutes) imagery from drones or shore-based video cameras. The difference is the dependence on the position of each wave breaker, similar to the unresolved phase of swash.

Overall, the discrepancy between the tracked and actual bar crest positions depends on several factors: (1) the accuracy of the sandbar tracking, (2) the pixel footprint, (3) photogrammetric errors mainly due to differences in actual elevation and tidal levels, and (4) tide- and wave-induced artificial shifts [13].

6. Discussion

Various factors have been investigated to understand the sudden accretion wave on the beach. These include changes in wave patterns (discounted due to stable observations in 2021), alterations in the sandspit (rare and occurring every 35 years), effects of riprap (which was completed after 2020), and sand waves originating from the Saharan desert coast. While regional features such as shoreline instabilities or anomaly-causing mechanisms may contribute, analysis of shoreline anomalies near the city reveals no antecedent features, suggesting a unique phenomenon in Saint Louis. Finally, an oil terminal with a 1 km breakwater was built 10 km offshore in 2021, which could also affect the shoreline. Is it responsible for attenuating the wave energy [58], making the conditions sufficient to control the bar and its splitting? The seasonality of the wave climate helps to understand the sandbar and, in turn, the position of the shoreline. Despite the erosion trend registered until 2020, the coast is strongly influenced by the wave climate, which varies enormously from the wet to the dry season. Thanks to the regular revisits of the Sentinel-2 satellites, a seasonal cycle of advance and retreat of the coastline can be detected. This behavior seems to be linked to a natural seasonal cycle of the coastline: it moves

seaward during the dry season—from November to April—and retreats during the wet season—from June to October (Figure 5).

The riprap, the construction of which began at the end of 2020, was the strategy chosen to protect the population rapidly from the dangers of the sea. The erosion recorded at Saint Louis, caused by the breach in the spit in 2003, was rapid (about −4.2 m/year [43]) and endangered the population living on the Langue de Barbarie, causing, for example, the collapse of buildings and the implementation of a resettlement plan [21,22,43]. Faced with this catastrophic situation, rockfill became an obvious choice: a protective measure had to be put in place as a matter of urgency. The accretion anomaly occurred during the construction of the protective structure, and the objective of the study was to understand the reason(s) for such a widening of the beach. However, despite the presence of the riprap, the accretion is due to the welding of the inner bar to the shoreline. In fact, the sandbar split during low-energy conditions (probably around the 2019 wet season, looking at both satellite images in Figure 4 and 2019 wet season wave conditions in Figure 3). According to the landward migration mechanisms of the bar described in [57], the remaining internal bar had slowly migrated to the shoreline and eventually gradually and completely welded to the beach during the 2020 wet season, resulting in the accretion of approximately 50 m of beach. In [13], the welding of a sandbar horn to the beach resulted in an accretion of approximately 100,000 m^3 for a cross-shore accretion feature of over 100 m along the same length of shoreline. Several other bar burst points were detected in the time series along the Langue de Barbarie coastline, far from the riprap influence zone, proving that beach nourishment by the sandbar is the phenomenon responsible for beach accretion.

Looking at the satellite images, both the sandbar and the shoreline appear to be linear rather than three-dimensional. However, since the satellite resolution is 10 m/pixel, the longshore variability of the sandbar is not investigated in this work. The accretion recorded around 2020 is not uniform across the region. On snapshot 2, Figure 4, the sandbar is welded to the shore. The waves, whose direction is NNW, cause the rest of the sandbar to migrate shoreward south of this point: the region where beach accretion is observed.

This study highlights the advantages of using satellite tools to monitor sandbars and coastal morphology. The splitting of sandbars is difficult to detect at the local scale (a few tens of meters) or almost impossible to detect if the splitting phenomenon does not occur in the field of view of the camera, as is the case with shoreward propagating accretive waves ([13,59–61]) or with in situ measurements, which are less frequent and miss some of the high-frequency coastal events and variability ([62]). This makes a clear case for the inclusion of satellite monitoring in coastal monitoring strategies [17,18], as a complement to high-frequency video monitoring and in situ measurements. This is the only way forward if we are to understand the relationship between (1) the foreshore and the aerial beach [63] and (2) between local and regional scales, both of which are critical for science-based decision making and effective management strategies [64]. As ground-based observations are generally lacking in Africa, these open-access satellite data are a game changer [36] but also elsewhere [65].

7. Conclusions

In conclusion, this study highlights the critical role of sandbar dynamics in shaping beach morphology, particularly in the context of coastal management strategies. Using Sentinel-2 satellite imagery, we have demonstrated the strong coupled behavior between the beach of Saint Louis, Senegal, and its adjacent sandbars, highlighting the significant influence of sandbar migration on coastal change. In particular, the observed 50 m beach accretion in 2020 was directly related to local welding of the inner sandbar to the shoreline, a phenomenon that could be anticipated in the future with prior sandbar analysis and monitoring.

While manual digitization of sandbar positions using wave-induced foam is an established technique, its application in this study with a high degree of accuracy in a challenging coastal environment is a notable achievement. Furthermore, the integration of Google Earth

Engine (GEE) for processing large volumes of satellite imagery represents a significant methodological advancement. This approach allows for efficient analysis of spatial data over extended time scales, surpassing the capabilities of traditional field-based methods.

However, despite the validation using the 2019 topo-bathymetry dataset, this study also highlights the need for more frequent and extensive validation efforts to mitigate the uncertainties associated with satellite-derived data. Future research should focus on strengthening these validation processes to further improve the accuracy and reliability of satellite-based coastal monitoring, ultimately supporting more informed and effective coastal management practices.

Author Contributions: Conceptualization, A.T. and R.A.; methodology, A.T.; software, A.T.; validation, A.T. and R.A.; formal analysis, A.T.; investigation, A.T. and R.A.; resources, B.A.S., A.N. and C.O.T.C.; data curation, A.T.; writing—original draft preparation, A.T.; writing—review and editing, A.T., R.A. and E.W.J.B.; visualization, A.T.; supervision, R.A. and E.W.J.B. All authors have read and agreed to the published version of the manuscript.

Funding: This research received funding from the PPCS ADM/AFD project and was conducted within the framework of the WACA-VAR West Africa regional program.

Data Availability Statement: All the images used in this study can be found on GEE (Google Earth Engine).

Acknowledgments: This research was supported by the ANR-22-ASTR-0013-01 GLOBCOASTS project and the Coastal Protection Project in Saint-Louis (PPCS), funded by the Senegalese ADM and the French AFD.

Conflicts of Interest: The authors declare no conflicts of interest. The funders had no role in the design of the study; in the collection, analyses, or interpretation of data; in the writing of the manuscript; or in the decision to publish the results.

Abbreviations

The following abbreviations are used in this manuscript:

GEE	Google Earth Engine
RGB	Red–Green–Blue
SW	sandbar welding
STT	sandbar to terrace bar transition
TST	terrace bar to sandbar transition
SS	sandbar splitting
NOM	net offshore migration

References

1. Van Enckevort, I.; Ruessink, B. Video observations of nearshore bar behaviour. Part 1: Alongshore uniform variability. *Cont. Shelf Res.* **2003**, *23*, 501–512. [CrossRef]
2. Van Enckevort, I.; Ruessink, B.; Coco, G.; Suzuki, K.; Turner, I.; Plant, N.G.; Holman, R.A. Observations of nearshore crescentic sandbars. *J. Geophys. Res. Ocean.* **2004**, *109*. [CrossRef]
3. Castelle, B.; Bourget, J.; Molnar, N.; Strauss, D.; Deschamps, S.; Tomlinson, R. Dynamics of a wave-dominated tidal inlet and influence on adjacent beaches, Currumbin Creek, Gold Coast, Australia. *Coast. Eng.* **2007**, *54*, 77–90. [CrossRef]
4. Ribas, F.; Falqués, A.; Garnier, R. Nearshore sand bars. In *Atlas of Bedforms in the Western Mediterranean*; Springer: Berlin, Germany, 2017; pp. 73–79.
5. Wright, L.D.; Short, A.D. Morphodynamic variability of surf zones and beaches: A synthesis. *Mar. Geol.* **1984**, *56*, 93–118. [CrossRef]
6. Lippmann, T.C.; Holman, R.A. Quantification of sand bar morphology: A video technique based on wave dissipation. *J. Geophys. Res. Ocean.* **1989**, *94*, 995–1011. [CrossRef]
7. Lippmann, T.; Holman, R. The spatial and temporal variability of sand bar morphology. *J. Geophys. Res. Ocean.* **1990**, *95*, 11575–11590. [CrossRef]
8. Stive, M.J.; Aarninkhof, S.G.; Hamm, L.; Hanson, H.; Larson, M.; Wijnberg, K.M.; Nicholls, R.J.; Capobianco, M. Variability of shore and shoreline evolution. *Coast. Eng.* **2002**, *47*, 211–235. [CrossRef]

9. Ruessink, B.; Kuriyama, Y.; Reniers, A.; Roelvink, J.; Walstra, D. Modeling cross-shore sandbar behavior on the timescale of weeks. *J. Geophys. Res. Earth Surf.* **2007**, *112*. [CrossRef]
10. Castelle, B.; Ruessink, B.; Bonneton, P.; Marieu, V.; Bruneau, N.; Price, T.D. Coupling mechanisms in double sandbar systems. Part 1: Patterns and physical explanation. *Earth Surf. Process. Landforms* **2010**, *35*, 476–486. [CrossRef]
11. Bouvier, C.; Castelle, B.; Balouin, Y. Modeling the impact of the implementation of a submerged structure on surf zone sandbar dynamics. *J. Mar. Sci. Eng.* **2019**, *7*, 117. [CrossRef]
12. Ruessink, B.; Pape, L.; Turner, I. Daily to interannual cross-shore sandbar migration: Observations from a multiple sandbar system. *Cont. Shelf Res.* **2009**, *29*, 1663–1677. [CrossRef]
13. Almar, R.; Castelle, B.; Ruessink, B.; Sénéchal, N.; Bonneton, P.; Marieu, V. Two-and three-dimensional double-sandbar system behaviour under intense wave forcing and a meso–macro tidal range. *Cont. Shelf Res.* **2010**, *30*, 781–792. [CrossRef]
14. Dubarbier, B.; Castelle, B.; Marieu, V.; Ruessink, G. Process-based modeling of cross-shore sandbar behavior. *Coast. Eng.* **2015**, *95*, 35–50. [CrossRef]
15. Aleman, N.; Certain, R.; Robin, N.; Barusseau, J.P. Morphodynamics of slightly oblique nearshore bars and their relationship with the cycle of net offshore migration. *Mar. Geol.* **2017**, *392*, 41–52. [CrossRef]
16. Shand, R.D. Relationships between episodes of bar switching, cross-shore bar migration and outer bar degeneration at Wanganui, New Zealand. *J. Coast. Res.* **2003**, *19*, 157–170.
17. Melet, A.; Teatini, P.; Le Cozannet, G.; Jamet, C.; Conversi, A.; Benveniste, J.; Almar, R. Earth Observations for Monitoring Marine Coastal Hazards and Their Drivers. *Surv. Geophys.* **2020**, *41*, 1489–1534. [CrossRef]
18. Benveniste, J.; Cazenave, A.; Vignudelli, S.; Fenoglio-Marc, L.; Shah, R.; Almar, R.; Andersen, O.; Birol, F.; Bonnefond, P.; Bouffard, J.; et al. Requirements for a Coastal Hazards Observing System. *Front. Mar. Sci.* **2019**, *6*, 348. [CrossRef]
19. Salameh, E.; Frappart, F.; Almar, R.; Baptista, P.; Heygster, G.; Lubac, B.; Raucoules, D.; Almeida, L.P.; Bergsma, E.W.J.; Capo, S.; et al. Monitoring Beach Topography and Nearshore Bathymetry Using Spaceborne Remote Sensing: A Review. *Remote Sens.* **2019**, *11*, 2212. [CrossRef]
20. Bergsma, E.; Sadio, M.; Sakho, I.; Almar, R.; Garlan, T.; Gosselin, M.; Gauduin, H. Sand-spit evolution and inlet dynamics derived from space-borne optical imagery: Is the Senegal-river inlet closing? *J. Coast. Res.* **2020**, *95*, 372–376. [CrossRef]
21. Ndour, A.; Ba, K.; Almar, A.; Almeida, P.; Sall, M.; Diedhiou, P.; Floc'h, F.; Daly, C.; Grandjean, P.; Boivin, J.P.; et al. On the natural and anthropogenic drivers of the Senegalese (West Africa) low coast evolution: Saint Louis Beach 2016 COASTVAR experiment and 3D modeling of short term coastal protection measures. *J. Coast. Res.* **2020**, *95*, 583–587. [CrossRef]
22. Sadio, M.; Anthony, E.J.; Diaw, A.T.; Dussouillez, P.; Fleury, J.T.; Kane, A.; Almar, R.; Kestenare, E. Shoreline Changes on the Wave-Influenced Senegal River Delta, West Africa: The Roles of Natural Processes and Human Interventions. *Water* **2017**, *9*, 357. [CrossRef]
23. Valentini, N.; Saponieri, A.; Molfetta, M.G.; Damiani, L. New algorithms for shoreline monitoring from coastal video systems. *Earth Sci. Inform.* **2017**, *10*, 495–506. [CrossRef]
24. Plant, N.G.; Aarninkhof, S.G.; Turner, I.L.; Kingston, K.S. The performance of shoreline detection models applied to video imagery. *J. Coast. Res.* **2007**, *23*, 658–670. [CrossRef]
25. Luijendijk, A.; Hagenaars, G.; Ranasinghe, R.; Baart, F.; Donchyts, G.; Aarninkhof, S. The state of the world's beaches. *Sci. Rep.* **2018**, *8*, 6641. [CrossRef]
26. Vos, K.; Splinter, K.D.; Harley, M.D.; Simmons, J.A.; Turner, I.L. CoastSat: A Google Earth Engine-enabled Python toolkit to extract shorelines from publicly available satellite imagery. *Environ. Model. Softw.* **2019**, *122*, 104528. [CrossRef]
27. Cabezas-Rabadán, C.; Almonacid-Caballer, J.; Benavente, J.; Castelle, B.; Del Río, L.; Montes, J.; Palomar-Vázquez, J.; Pardo-Pascual, J.E. Assessing Satellite-Derived Shoreline Detection on a Mesotidal Dissipative Beach. *Remote Sens.* **2024**, *16*, 617. [CrossRef]
28. Bergsma, E.W.; Klotz, A.N.; Artigues, S.; Graffin, M.; Prenowitz, A.; Delvit, J.M.; Almar, R. Shoreliner: A Sub-Pixel Coastal Waterline Extraction Pipeline for Multi-Spectral Satellite Optical Imagery. *Remote Sens.* **2024**, *16*, 2795. [CrossRef]
29. Almeida, L.P.; de Oliveira, I.E.; Lyra, R.; Dazzi, R.L.S.; Martins, V.G.; da Fontoura Klein, A.H. Coastal analyst system from space imagery engine (CASSIE): Shoreline management module. *Environ. Model. Softw.* **2021**, *140*, 105033. [CrossRef]
30. Mentaschi, L.; Vousdoukas, M.I.; Pekel, J.F.; Voukouvalas, E.; Feyen, L. Global long-term observations of coastal erosion and accretion. *Sci. Rep.* **2018**, *8*, 12876. [CrossRef]
31. Pardo-Pascual, J.E.; Sánchez-García, E.; Almonacid-Caballer, J.; Palomar-Vázquez, J.M.; Priego De Los Santos, E.; Fernández-Sarría, A.; Balaguer-Beser, Á. Assessing the accuracy of automatically extracted shorelines on microtidal beaches from Landsat 7, Landsat 8 and Sentinel-2 imagery. *Remote Sens.* **2018**, *10*, 326. [CrossRef]
32. Holman, R.; Stanley, J. The history and technical capabilities of Argus. *Coast. Eng.* **2007**, *54*, 477–491. [CrossRef]
33. Lippmann, T.C.; Smith, G.M. Shallow Surveying in Hazardous Waters. In Proceedings of the U.S. Hydrographic Conference, Norfolk, VA, USA, 11–14 May 2009; pp. 1–12.
34. Almar, R.; Bonneton, P.; Senechal, N.; Roelvink, D. Wave celerity from video imaging: A new method. In *Coastal Engineering 2008: (In 5 Volumes)*; World Scientific: Singapore, 2009; pp. 661–673.
35. Turner, I.L.; Harley, M.D.; Almar, R.; Bergsma, E.W.J. Satellite optical imagery in Coastal Engineering. *Coast. Eng.* **2021**, *167*, 103919. [CrossRef]

36. Almar, R.; Stieglitz, T.; Addo, K.A.; Ba, K.; Ondoa, G.A.; Bergsma, E.W.; Bonou, F.; Dada, O.; Angnuureng, D.; Arino, O. Coastal zone changes in West Africa: Challenges and opportunities for satellite earth observations. *Surv. Geophys.* **2023**, *44*, 249–275. [CrossRef]
37. Lafon, V.; Apoluceno, D.D.M.; Dupuis, H.; Michel, D.; Howa, H.; Froidefond, J.M. Morphodynamics of nearshore rhythmic sandbars in a mixed-energy environment (SW France): I. Mapping beach changes using visible satellite imagery. *Estuar. Coast. Shelf Sci.* **2004**, *61*, 289–299. [CrossRef]
38. Zhang, X.; Wu, C.; Zhang, Y.; Hu, R.; Yang, Z. Using free satellite imagery to study the long-term evolution of intertidal bar systems. *Coast. Eng.* **2022**, *174*, 104123. [CrossRef]
39. Do, J.D.; Jin, J.Y.; Jeong, W.M.; Lee, B.; Kim, C.H.; Chang, Y.S. Observation of nearshore crescentic sandbar formation during storm wave conditions using satellite images and video monitoring data. *Mar. Geol.* **2021**, *442*, 106661. [CrossRef]
40. Janušaitė, R.; Jukna, L.; Jarmalavičius, D.; Pupienis, D.; Žilinskas, G. A novel GIS-based approach for automated detection of nearshore sandbar morphological characteristics in optical satellite imagery. *Remote Sens.* **2021**, *13*, 2233. [CrossRef]
41. Tătui, F.; Constantin, S. Nearshore sandbars crest position dynamics analysed based on Earth Observation data. *Remote Sens. Environ.* **2020**, *237*, 111555. [CrossRef]
42. Davidson, M.; Van Koningsveld, M.; de Kruif, A.; Rawson, J.; Holman, R.; Lamberti, A.; Medina, R.; Kroon, A.; Aarninkhof, S. The CoastView project: Developing video-derived Coastal State Indicators in support of coastal zone management. *Coast. Eng.* **2007**, *54*, 463–475. [CrossRef]
43. Ndour, A.; Laïbi, R.A.; Sadio, M.; Degbe, C.G.; Diaw, A.T.; Oyédé, L.M.; Anthony, E.J.; Dussouillez, P.; Sambou, H.; hadji Balla Dièye, E. Management strategies for coastal erosion problems in west Africa: Analysis, issues, and constraints drawn from the examples of Senegal and Benin. *Ocean. Coast. Manag.* **2018**, *156*, 92–106. [CrossRef]
44. Cisse, C.O.T.; Brempong, E.; Taveneau, A.; Almar, R.; Sy, B.A.; Angnuureng, D.B. Extreme coastal water levels with potential flooding risk at the low-lying Saint Louis historic city, Senegal (West Africa). *Front. Mar. Sci.* **2022**, *9*, 993644. [CrossRef]
45. Almar, R.; Kestenare, E.; Boucharel, J. On the key influence of remote climate variability from Tropical Cyclones, North and South Atlantic mid-latitude storms on the Senegalese coast (West Africa). *Environ. Res. Commun.* **2019**, *1*, 071001. [CrossRef]
46. Anthony, E. Patterns of Sand Spit Development and Their Management Implications on Deltaic, Drift-Aligned Coasts: The Cases of the Senegal and Volta River Delta Spits, West Africa. In *Sand and Gravel Spits*; Randazzo, G., Jackson, D., Cooper, J., Eds.; Coastal Research Library; Springer: Cham, Switzerland, 2015; pp. 21–36.
47. Taveneau, A.; Almar, R.; Bergsma, E.W.J.; Sy, B.A.; Ndour, A.; Sadio, M.; Garlan, T. Observing and Predicting Coastal Erosion at the Langue de Barbarie Sand Spit around Saint Louis (Senegal, West Africa) through Satellite-Derived Digital Elevation Model and Shoreline. *Remote Sens.* **2021**, *13*, 2454. [CrossRef]
48. Rodríguez, S.; Alonso Bilbao, I.; Sánchez García, M.J.; Casamayor Font, M.; García Weil, L.F.; Sy, B.; Sy, A.; Faye, C. Morphodynamic study of an artificial inlet in Langue de Barbarie (Senegal) from 2003 to 2014 using Landsat images. In Proceedings of the IV Congress of Marine Sciences, Las Palmas de Gran Canaria, Spain, 11–13 June 2014.
49. Dean, R.; Dalrymple, R. Long-term processes. In *Coastal Processes with Engineering Applications*; Cambridge University Press: Cambridge, UK, 2001; pp. 35–70.
50. Aubrey, D.; Gaines, A. Rapid formation and degradation of barrier spits in areas with low rates of littoral drift. *Mar. Geol.* **1982**, *49*, 257–277. [CrossRef]
51. Bergsma, E.W.; Almar, R. Coastal coverage of ESA' Sentinel 2 mission. *Adv. Space Res.* **2020**, *65*, 2636–2644. [CrossRef]
52. Van Enckevort, I.; Ruessink, B. Effect of hydrodynamics and bathymetry on video estimates of nearshore sandbar position. *J. Geophys. Res. Ocean.* **2001**, *106*, 16969–16979. [CrossRef]
53. Pape, L.; Ruessink, B. Multivariate analysis of nonlinearity in sandbar behavior. *Nonlinear Process. Geophys.* **2008**, *15*, 145–158. [CrossRef]
54. Hersbach, H.; Bell, B.; Berrisford, P.; Hirahara, S.; Horányi, A.; Muñoz-Sabater, J.; Nicolas, J.; Peubey, C.; Radu, R.; Schepers, D.; et al. The ERA5 global reanalysis. *Q. J. R. Meteorol. Soc.* **2020**, *146*, 1999–2049. [CrossRef]
55. Pereira, D. Wind Rose: MATLAB Central File Exchange. Available online: https://fr.mathworks.com/matlabcentral/fileexchange/47248-wind-rose (accessed on 23 November 2021).
56. Garlan, T.; Almar, R.; Gauduin, H.; Gosselin, M.; Morio, O.; Labarthe, C. 3D variability of sediment granulometry in two tropical environments: Nha Trang (Vietnam) and Saint-Louis (Senegal). *J. Coast. Res.* **2020**, *95*, 495–499. [CrossRef]
57. Vidal-Ruiz, J.A.; de Alegría-Arzaburu, A.R. Modes of onshore sandbar migration at a single-barred and swell-dominated beach. *Mar. Geol.* **2020**, *426*, 106222. [CrossRef]
58. Alari, V.; Raudsepp, U. Simulation of wave damping near coast due to offshore wind farms. *J. Coast. Res.* **2012**, *28*, 143–148. [CrossRef]
59. Price, T.D.; Ruessink, B.G.; Castelle, B. *Morphological Coupling in a Double Sandbar System*; Utrecht University: Utrecht, The Netherlands, 2013.
60. Price, T.; van Kuik, N.; de Wit, L.; Dionísio António, S.; Ruessink, B. Shoreward propagating accretionary waves (SPAWs): Observations from a multiple sandbar system. In Proceedings of the Coastal Dynamics 2017, Helsingør, Denmark, 12–16 June2017; pp. 1081–1089.
61. Wijnberg, K.M.; Holman, R. Video-observations of shoreward propagating accretionary waves. *Proc. RCEM* **2007**, *2007*, 737–743.

62. Bergsma, E.W.; Almar, R.; Anthony, E.J.; Garlan, T.; Kestenare, E. Wave variability along the world's continental shelves and coasts: Monitoring opportunities from satellite Earth observation. *Adv. Space Res.* **2022**, *69*, 3236–3244. [CrossRef]
63. Anthony, E.J.; Aagaard, T. The lower shoreface: Morphodynamics and sediment connectivity with the upper shoreface and beach. *Earth-Sci. Rev.* **2020**, *210*, 103334. [CrossRef]
64. Alves, B.; Angnuureng, D.B.; Morand, P.; Almar, R. A review on coastal erosion and flooding risks and best management practices in West Africa: What has been done and should be done. *J. Coast. Conserv.* **2020**, *24*, 1–22. [CrossRef]
65. Vitousek, S.; Buscombe, D.D.; Vos, K.; Barnard, P.; Ritchie, A.; Warrick, J. The future of coastal monitoring through satellite remote sensing. *Camb. Prism. Coast. Futures* **2023**, *1*, e10. [CrossRef]